ROBUST SEGMENTATION OF CLINICAL OPTIC NERVE MRI

Swetasudha Panda[1], Andrew J Asman[1], Bennett A Landman[1,2], Seth A Smith[2], and Louise A Mawn[3]

[1]Electrical Engineering, Vanderbilt University, Nashville, TN, United States, [2]Radiology and Radiological Sciences, Vanderbilt University, Nashville, TN, United States, [3]Ophthalmology and Neurological Surgery, Vanderbilt University, Nashville, TN, United States

Target Audience: Physicists and clinicians focused on developing novel MRI-based tools to characterize small nervous system structures.

Purpose: The optic nerve (ON) is a central player not only in processing and relaying visual information from the eye, but also in in devastating pathological conditions such as optic neuritis, multiple sclerosis (MS) and optic nerve head drusen (ONHD). As with other central nervous system structures, pathology has shown that the optic nerve can undergo many changes in the course of disease not limited to: inflammation, atrophy, axonal congestion, yet many MRI-based tools have struggled to characterize the extent of the optic nerve's involvement in central nervous system (CNS) diseases. Thus, our purpose is to develop tools to automatically quantify the location and volumetrics of the optic nerve which promises to provide integration of multi-modal imaging data. We hypothesize that this will increase sensitivity and specificity of pathology assessments relative to coarse, manual region of interest approaches. Additionally manual segmentation struggles significantly in the optic nerve when pathology is present or in the later stages of optic nerve damage. While multi-atlas segmentation promises a robust and model-free approach to segment medical images from exemplar images for brain structures, extrapolation to smaller structures of the human anatomy have largely been unexplored. Our purpose is to extend and evaluate multi-atlas labeling for the segmentation of the ON based on high-resolution T2-weighted MRI of the optic nerve.

Theory: Non-rigid registration is performed on Regions of Interests (ROIs) localized for the target and atlas images using the ON centroid results from the initial rigid registration. Non-Local STAPLE (NLS) for label fusion provides a novel approach for accounting for consistent registration errors and bias within the traditional STAPLE estimation framework. In order to accomplish this, NLS incorporates the theory of non-local means [1]. This approach deconstructs image volumes into a collection of small volumetric patches and the similarity (or correspondence) is quantified in order to learn information about the underlying image structure.

Methods: We performed T2-weighted VISTA (3D Spin Echo with asymmetric k-space turbo spin echo readout, TR/TE = 4s/400ms, nominal resolution = $0.6mm^3$ isotropic, 50 axial slices, SENSE = 2, body coil excitation, 32 channel receive coil, and total scan time = 4.3 min) 3T (Philips Medical Systems) MRI of the optic nerves from the globe to the chiasm in 36 subjects (32 controls, 4 MS patients and 2 ONHD patients). Manual segmentation was performed using the MIPAV software package for the full length of the optic nerve on 10 randomly selected control datasets to obtain 10 pairs of images and labels (i.e., the "atlases"). The remaining 26 datasets were labeled using the NLS segmentation algorithm based on the 10 atlases [2]. Briefly, pairwise non-rigid registration was performed for all atlas images and targets using the VABRA module in JIST [3]. All the atlas labels were transformed to the coordinate space of each target with nearest neighbour interpolation. Non-local statistical fusion was used to reconcile inconsistencies in labels and form a single segmentation estimate. To evaluate this automated segmentation method, we manually segmented the full optic nerve volumes on 4 of the automatically segmented images (1 control, 1 MS patient, and 2 ONHD patients) and 100 randomly selected coronal slices from the remaining 26 datasets. We report the difference in CSA on coronal sections, the Hausdorff distance (maximum surface distance) for each pair of manual and automatic segmented slice (within slices), and Dice Similarity Coefficient (DSC).

Results and Discussion: For the 4 fully segmented subjects (8 optic nerves, **Figure 1**), the mean differences in the CSA for the manual and automatic pairs of volumes were 1.4, 1.5, 6.2 and 2.6 mm^2 respectively. The mean DSCs were 0.72, 0.76, 0.70 and 0.61 respectively. The Hausdorff distances were 3.8, 4.89, 1.54 and 2.19 mm respectively and the mean surface distances were 0.5237, 0.4847, 0.5021 and 0.5590 mm. For the 100 random slices, the mean Hausdorff distance between the corresponding pairs was 1.24 mm and DSC was 0.78. The mean difference in CSA over these 100 slices was 5.58 mm^2 for the left optic nerve and 4.21 mm^2 for the right optic nerve. We note that the accuracy of manual segmentation of randomly selected slices is lower given reduced 3D context which would explain the increased disparity in the control slices versus the comprehensive segmentations.

Conclusions: Multi-atlas segmentation provides a robust approach to obtain volumetric information even in patients where significant atrophy is present (ONHD patients) and when inflammation is easily appreciated (MS patients) using atlases based only on healthy controls. The automated segmentations could be used to provide analysis context (i.e., navigation), volumetric assessment, or enable regional nerve characterization (i.e., localize changes). We note that the current assessment approach occasionally results in large maximal distances when considering only within-slice error (spikes in Figure 1). This is a result of minor failures in the automatic segmentations which could be resolved with more stringent 3-D consistency (i.e., Markov Random Field regularization) or tubular structure enforcement [4]. We further propose the opportunity to obtain high-fidelity volumetric analysis in patient populations will provide for the first time a routine clinical method to correlate ophthalmological findings with radiological imaging, a task that to date, has not been offered in the clinical assessment of patients with optic nerve pathology.

References: [1] Buades, Coll, Morel (2005) (CVPR) 2, 60-65. [2] Asman and Landman (2012). LNCS. Vol 7512, pp 426-434. [3] Rohde, Aldroubi, Dawant. (2003) IEEE TMI. **22**(11): p. 1470-9. [4] Noble and Dawant (2011) MedIA, 15(6), 877-84.
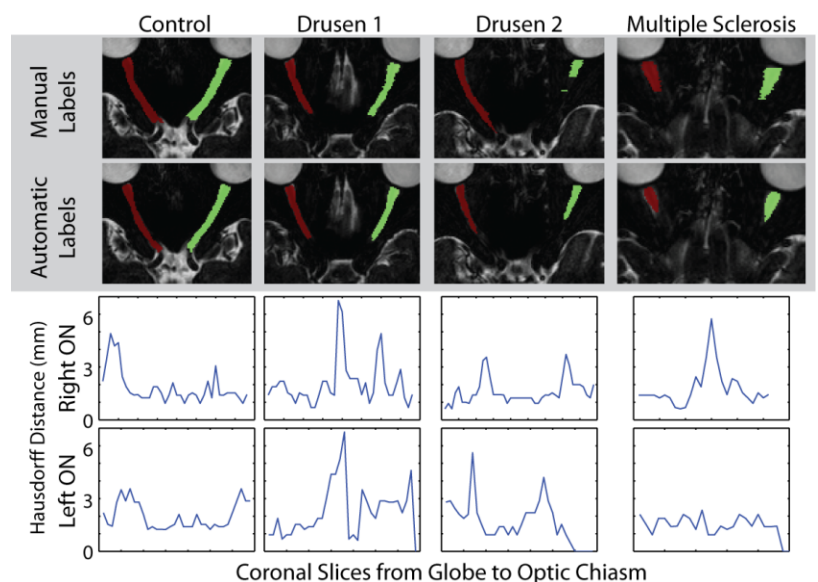
Figure 1. Comparison of manual and automated segmentation of the optic nerve on four subjects. The right optic nerve is shown in red and the left in green in the top two plots. The lower plots show the maximum slice-wise surface distance between the respective automatic and manual segmentations.